doi:10.1246/cl.2012.1319
Published on the web October 20, 2012

A Strategy for Amorphous Arrangement of Gold Nanoparticles Using Eccentric Hybrid Particles

Akira Ohnuma,*[1,2,3] Eun Chul Cho,[2,4] and Bunsho Ohtani[1]
[1]*Catalysis Research Center, Hokkaido University, Sapporo, Hokkaido 001-0021*
[2]*Department of Biomedical Engineering, Washington University, St. Louis, Missouri 63130, USA*
[3]*Institute for the Advancement of Higher Education, Hokkaido University, Sapporo, Hokkaido 060-0817*
[4]*Department of Chemical Engineering, Division of Chemical and Bioengineering, Hanyang University, Seoul 133-791, Korea*

(Received May 14, 2012; CL-120606; E-mail: ohnuma@high.hokudai.ac.jp)

Herein, we report a strategy to fabricate a three-dimensional amorphous arrangement of gold nanoparticles from eccentric gold–polymer hybrid particles. The arrangement of the gold nanoparticles in the three-dimensional colloidal lattice of the hybrid particles was amorphous because of the disordered orientation of the gold nanoparticles in each polymer bead. The amorphous arrangement was different from ordinary random structures, since it had a particular short-range order. Such an amorphous arrangement should have the potential for use in a new class of functional materials.

Designing more diverse structures with colloidal particles is of great interest owing to their possible applications, for example, in optical devices;[1–6] monodisperse colloidal spheres have been investigated as building blocks to fabricate photonic crystals with face-centered cubic (*fcc*), hexagonal close-packing (*hcp*), or other special symmetries such as diamond structures.[7–13] Besides that, there has been essentially no report on the fabrication of three-dimensional (3D) colloidal lattices lacking orientational order. For the fabrication of such a colloidal lattice, monodisperse noncentrosymmetric colloidal particles must be assembled with a coefficient of variation (CV) of less than 8%,[14,15] but it is technically difficult to prepare such uniform noncentrosymmetric particles, and disordered structures might be favorable for anisotropic particles owing to the increased entropy by the orientational freedom of the particle in suspension.[16]

Herein, we report a new class of 3D amorphous arrangements of Au nanoparticles from Au–polystyrene (PS) hybrid particles with an eccentric structure. The hybrid particles had an overall spherical shape and were uniform in size (CV < 5%). Each PS bead contained a Au nanoparticle.[17,18] The Au nanoparticles were offset from the center of the PS bead, being positioned very close to the surface. When the eccentric Au–PS particles were self-assembled, the Au nanoparticles were arranged in a disordered fashion, and such a structure can be considered as a "3D amorphous arrangement." Interestingly, the colloidal lattice displayed a Bragg diffraction peak in addition to the localized surface plasmon resonance (LSPR) feature of the Au nanoparticles.

Au–PS hybrid particles with an eccentric structure were prepared according to a previously described procedure[17,18] and then assembled into 3D colloidal lattices using a packing cell demonstrated by Xia et al.[19] (see Supporting Information[30]). The structure of the colloidal lattices was characterized using electron microscopes, and the optical property was investigated using spectrophotometers.

Figure 1 shows the TEM images of two samples of eccentric Au–PS particles that were used for the fabrication of 3D colloidal lattices. We used 50-nm Au nanoparticles for these syntheses. The diameters of the eccentric particles were controlled by varying the polymerization time (t) of PS: the average hydrodynamic diameters of the particles (measured using a particle size analyzer) were 210 nm at $t = 45$ min (Figure 1a) and 390 nm at $t = 4$ h (Figure 1b). The position of the Au nanoparticle in the PS bead can be varied by controlling the concentration of the crosslinker (divinylbenzene (DVB)). In the present study, we adjusted the concentration of DVB to 1.7 wt % to ensure that the Au nanoparticle would not protrude from the surface of the PS bead but would be very close to the surface. Because of their spherical shape and small size variation, the eccentric particles could serve as building blocks to fabricate colloidal lattices. The optical properties of these lattices are expected to be different from those assembled from pure silica or polymer beads, because of the presence of Au nanoparticles.[20–26]

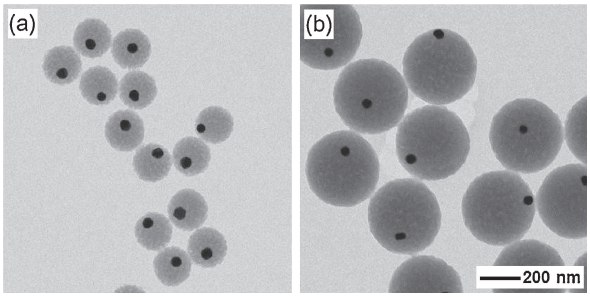

Figure 1. TEM images of eccentric Au–PS particles with different sizes that were prepared with a mixture of styrene and DVB (98.3:1.7 by weight). The average hydrodynamic diameters of the eccentric particles were (a) 210 and (b) 390 nm, respectively. For both samples, we used Au nanoparticles of 50 nm in diameter. The 200 nm scale bar applies to both images.

Figure 2 shows the SEM images of colloidal lattices assembled from the 210-nm and 390-nm eccentric particles. Both samples displayed an *fcc* structure for the PS beads with the (111) planes oriented parallel to the surfaces of the glass substrates. From the back-scattering SEM images shown in the insets, it can be clearly seen that the Au nanoparticles in the PS beads were disordered in the lattice structure. Before the assembly of the hybrid particles, it could not be predicted whether the Au nanoparticles would be aligned or not, but this result implied that the Brownian motion inherent to the colloidal particles tends to keep them oriented randomly in the aqueous dispersion until the spatial orientation of each particle is fixed in the colloidal lattice. From the brightness of the Au nanoparticles in the SEM images, it could be roughly stated that each Au nanoparticle is located at the top or bottom of the PS bead, and

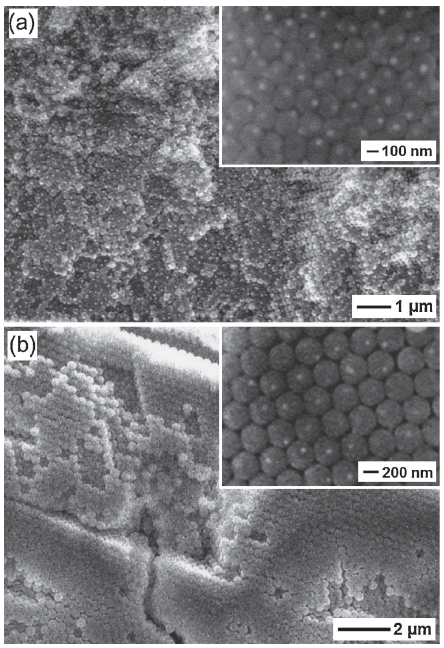

Figure 2. SEM images of colloidal lattices assembled from the (a) 210-nm and (b) 390-nm eccentric Au–PS particles, respectively. Both samples display a *fcc* structure for the PS beads with the (111) planes oriented parallel to the surface of the substrate. The insets are back-scattering SEM images, showing the alignment of the Au nanoparticles in the PS beads. It is clear that the Au nanoparticles were arranged in a disorderly manner.

the estimated ratios obtained from both samples were close to 1:1. The overall structure should lack orientational order or periodicity owing to such a disordered arrangement of the Au nanoparticles, and it can be considered as a "3D amorphous arrangement." The arrangement is different from ordinary random structures, since it has a short-range order in which the distance between the centers of neighboring Au nanoparticles is always shorter than twice the diameter of the hybrid particles, and each Au nanoparticle is constantly surrounded by 12 other neighbor nanoparticles. Fabrication of the *fcc* lattice from hybrid particles is only the way to obtain such an amorphous arrangement. It is worth noting that the colloidal lattice could be successfully formed from noncentrosymmetric particles in a fashion similar to ordinary spherical particles, in spite of their noncentral gravity points, which are located at 15 nm (14% of the radius) and 6 nm (3% of the radius) off the center for the 210-nm and 390-nm eccentric particles, respectively.

Next, the optical properties of the aqueous dispersions of the eccentric particles and their colloidal lattices were investigated using a UV–vis spectrophotometer. Figure 3a shows the absorption spectra recorded for the two samples of eccentric particles dispersed in water. Since the refractive index of PS is higher than that of water (1.60 vs. 1.33), the LSPR peak of the 50-nm Au nanoparticles in the eccentric particles was red-shifted from the original position at 530 to 550 nm upon the incorporation of Au nanoparticles in PS. Figure 3b shows the transmission spectra recorded with the lattices assembled from 210-nm and 390-nm eccentric particles in packing cells of 2.5 and 6 μm thickness, respectively. When recording the spectra, the void spaces among the particles were still filled with water.

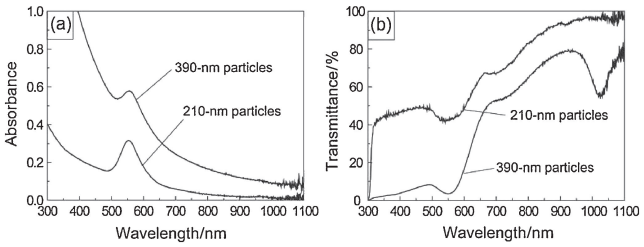

Figure 3. (a) UV–vis absorption spectra taken from aqueous dispersions of the 210-nm and 390-nm eccentric Au–PS particles. (b) UV–vis transmission spectra recorded from colloidal lattices assembled from the 210-nm and 390-nm eccentric Au–PS particles, respectively. The transmission spectra were recorded while the incident light was oriented perpendicular to the surface of the glass substrate. The samples were filled with water to completely wet the void spaces in the lattices.

The transmission spectra are supposed to show two characteristic peaks, the LSPR peak of the Au nanoparticles (ca. 550 nm) and the Bragg diffraction peak associated with the 3D lattice. We could clearly resolve the two peaks for the lattice constructed from the 390-nm eccentric particles. However, for the lattice assembled from the 210-nm particles, only one broad peak was observed at ca. 560 nm, because of the overlap of the LSPR and Bragg peaks.

The peak due to Bragg diffraction can be quantitatively analyzed using the following equation:[27,28]

$$m\lambda_{\max} = 2d_{hkl}(n^2 - \sin^2\theta)^{1/2} \quad (1)$$

where m is the order of diffraction; d_{hkl}, the spacing between (hkl) planes; n, the refractive index of the lattice; and θ, the angle between the incident light and the surface of the diffraction planes ($\theta = 0°$ in our measurements). For the *fcc* lattice, $d_{111} = 4r/(6)^{1/2}$, where r is the radius of the eccentric particles ($r = 105$ or 195 nm). Since the average position of the Au nanoparticles can be considered as the center of the PS beads, it is reasonable to calculate the refractive index (n) in the same way as that for the colloidal crystals assembled from core–shell particles in which the core particle is located at the center. The n value of the eccentric Au–PS particles can be calculated according to the following equation by assuming a linear relationship between n and the volume fraction (X) of the eccentric particles:[29]

$$n_{\text{Au–PS(210 or 390 nm),particle}} = n_{\text{Au}}X_{\text{Au}} + n_{\text{PS}}X_{\text{PS}} \quad (2)$$

For the 210-nm eccentric particles, $n_{\text{Au}} = 0.47$, $X_{\text{Au}} = 0.014$, $n_{\text{PS}} = 1.6$, and $X_{\text{PS}} = 0.986$. On the other hand, for the 390-nm eccentric particles, $n_{\text{Au}} = 0.47$, $X_{\text{Au}} = 0.002$, $n_{\text{PS}} = 1.6$, and $X_{\text{PS}} = 0.998$. By substituting these parameters in eq 2, we obtained 1.58 and 1.60 as the average refractive indices of the 210-nm and 390-nm eccentric particles, respectively. The refractive index ($n_{\text{Au–PS,lattice}}$) for the opaline lattice from the 210-nm or 390-nm eccentric Au–PS particles can then be calculated according to the following equation:

$$n_{\text{Au–PS(210 or 390 nm),lattice}} = n_{\text{voids}}f_{\text{voids}} + n_{\text{Au–PS(210 or 390 nm),particle}}(1 - f_{\text{voids}}) \quad (3)$$

where n_{voids} is the refractive index of the voids. Since we filled the voids with water for all the samples, $n_{\text{voids}} = 1.33$ in our studies. f_{voids} is the volume fraction of the voids in the 3D lattice,

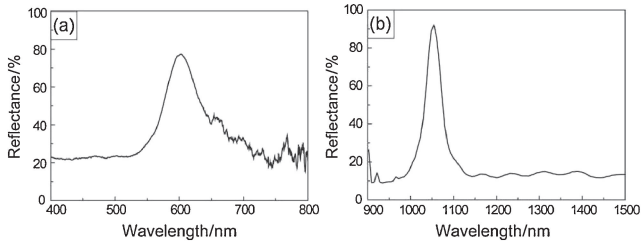

Figure 4. (a) UV–vis reflectance spectrum recorded for the colloidal lattice assembled from the 210-nm eccentric Au–PS particles in a 6 μm-thick packing cell. The spectrum was recorded with the incident/detection angle perpendicular to the surface of the glass substrates. (b) Near-infrared reflectance spectrum taken for the colloidal lattice assembled from the 390-nm eccentric Au–PS particles in a 76 μm-thick packing cell. The incident/detection angle was 10° from the normal to the surface of the glass substrate. Both samples were filled with water to completely wet the void spaces in the lattices.

and the value corresponds to 0.26 for an *fcc* structure. Therefore, eq 3 yields $n = 1.52$ and 1.53 for the crystalline lattices assembled from the 210-nm and 390-nm eccentric particles, respectively. The peak positions calculated from the Bragg equation are 521 and 974 nm, respectively. Although the experimental data were slightly red-shifted from the calculated values, they were basically consistent with the trend demonstrated by the red shift of the stop bands upon changing the sizes of the constituent particles. In this manner, the lattice assembled from the eccentric particles displayed peaks due to Bragg diffraction, but it should be mentioned that the Au nanoparticles do not play any significant role in the Bragg diffraction because of the small refractive index and low volume fraction (<2%) of the eccentric particles. A Fourier transform pattern from the back-scattering SEM image of the colloidal lattice was very similar to the hexagonal registry of the (111) crystallographic domains (Figure S1).[30] The unsharpness of the points on the reciprocal lattice might indicate the amorphous arrangement of the Au nanoparticles. On the other hand, it is worth noting that the peaks from the LSPR absorption of the Au nanoparticles have fairly strong intensity in spite of the low volume fractions.

Figure 4a shows the UV–vis reflectance spectrum recorded for the lattice assembled from the 210-nm eccentric particles in a 6-μm-thick packing cell, and Figure 4b shows the near-IR reflectance spectrum recorded for a lattice assembled from the 390-nm eccentric particles in a 76-μm-thick packing cell. When recording the spectra, the void spaces among the particles were filled with water. In this configuration, only Bragg diffraction peaks were detected, and no LSPR peaks were seen because of the weak scattering of Au nanoparticles in a specific direction. We also found that the peak positions were in agreement with those from the UV–vis transmission spectra. We further confirmed from the reflectance spectra that the colloidal lattice assembled with the 210-nm eccentric particles has a well-resolved Bragg diffraction peak that overlapped with the LSPR absorption peak from the Au nanoparticles in the transmission spectrum (Figure 4b).

In summary, we have demonstrated the fabrication of a novel 3D colloidal lattice by using Au–PS hybrid particles with an eccentric structure. The arrangement of the Au nanoparticles in the lattice was amorphous because of the disordered orientation of the Au nanoparticles in each PS bead. Because of the amorphous arrangement of the Au nanoparticles in the structure, it should be possible to use the colloidal lattice for a new class of functional materials. If the void spaces of the lattice are filled with materials showing the same refractive index as the PS beads, the Au nanoparticles will be optically floated in the structure, and an independent 3D amorphous structure of the Au nanoparticles could be obtained. Such a disordered arrangement might have unique optical properties different from those of normal ordered structures.

The authors thank Prof. Younan Xia for valuable discussions and Prof. Pedro H. C. Camargo for the experimental support. A.O. and B.O. acknowledge the MEXT Project of Integrated Research on Chemical Synthesis. E.C.C. acknowledges a Manpower Development Program for Energy (the Ministry of Knowledge and Economy, MKE).

Paper based on a presentation made at the International Association of Colloid and Interface Scientists, Conference (IACIS2012), Sendai, Japan, May 13–18, 2012.

References and Notes

1 S.-M. Yang, S.-H. Kim, J.-M. Lim, G.-R. Yi, *J. Mater. Chem.* **2008**, *18*, 2177.
2 K.-i. Okazaki, J.-i. Yasui, T. Torimoto, *Chem. Commun.* **2009**, 2917.
3 K. Sohn, F. Kim, K. C. Pradel, J. Wu, Y. Peng, F. Zhou, J. Huang, *ACS Nano* **2009**, *3*, 2191.
4 Y. Zhang, A. Barhoumi, J. B. Lassiter, N. J. Halas, *Nano Lett.* **2011**, *11*, 1838.
5 Y. I. Yang, E. Jeong, I. Choi, S. Lee, H. D. Song, K. Kim, Y. Choi, T. Kang, J. Yi, *Angew. Chem., Int. Ed.* **2011**, *50*, 4633.
6 E. Jeong, K. Kim, I. Choi, S. Jeong, Y. Park, H. Lee, S. H. Kim, L. P. Lee, Y. Choi, T. Kang, *Nano Lett.* **2012**, *12*, 2436.
7 Y. Xia, B. Gates, Y. Yin, Y. Lu, *Adv. Mater.* **2000**, *12*, 693.
8 A. Stein, R. C. Schroden, *Curr. Opin. Solid State Mater. Sci.* **2001**, *5*, 553.
9 C. López, *Adv. Mater.* **2003**, *15*, 1679.
10 Z. Zhang, A. S. Keys, T. Chen, S. C. Glotzer, *Langmuir* **2005**, *21*, 11547.
11 P. H. C. Camargo, Z.-Y. Li, Y. Xia, *Soft Mater* **2007**, *3*, 1215.
12 A. Ohnuma, R. Abe, T. Shibayama, B. Ohtani, *Chem. Commun.* **2007**, 3491.
13 M. Sadakane, R. Kato, T. Murayama, W. Ueda, *J. Solid State Chem.* **2011**, *184*, 2299.
14 R. Rengarajan, D. Mittleman, C. Rich, V. Colvin, *Phys. Rev. E: Stat., Nonlinear, Soft Matter Phys.* **2005**, *71*, 016615.
15 C. Paquet, M. Allard, G. Glédel, E. Kumacheva, *J. Phys. Chem. B* **2006**, *110*, 1605.
16 R. S. Berry, S. A. Rice, J. Ross, *Physical Chemistry*, 2nd ed., Oxford University Press, New York, **2000**.
17 A. Ohnuma, E. C. Cho, P. H. C. Camargo, L. Au, B. Ohtani, Y. Xia, *J. Am. Chem. Soc.* **2009**, *131*, 1352.
18 A. Ohnuma, E. C. Cho, M. Jiang, B. Ohtani, Y. Xia, *Langmuir* **2009**, *25*, 13880.
19 Y. Lu, Y. Yin, B. Gates, Y. Xia, *Langmuir* **2001**, *17*, 6344.
20 W. Wang, S. A. Asher, *J. Am. Chem. Soc.* **2001**, *123*, 12528.
21 K. P. Velikov, A. Moroz, A. van Blaaderen, *Appl. Phys. Lett.* **2002**, *80*, 49.
22 Y. Lu, Y. Yin, Z.-Y. Li, Y. Xia, *Nano Lett.* **2002**, *2*, 785.
23 L. M. Liz-Marzán, P. Mulvaney, *J. Phys. Chem. B* **2003**, *107*, 7312.
24 Y. Tan, W. Qian, S. Ding, Y. Wang, *Chem. Mater.* **2006**, *18*, 3385.
25 J. Huang, F. Kim, A. R. Tao, S. Connor, P. Yang, *Nat. Mater.* **2005**, *4*, 896.
26 J. Huang, A. R. Tao, S. Connor, R. He, P. Yang, *Nano Lett.* **2006**, *6*, 524.
27 I. I. Tarhan, G. H. Watson, *Phys. Rev. B* **1996**, *54*, 7593.
28 S. H. Park, Y. Xia, *Langmuir* **1999**, *15*, 266.
29 H. Takeda, K. Yoshino, *Appl. Phys. Lett.* **2002**, *80*, 4495.
30 Supporting Information is available electronically on the CSJ-Journal Web site, http://www.csj.jp/journals/chem-lett/index.html.

